AlScN: A III-V semiconductor based ferroelectric 🅕 ✅

Simon Fichtner (ID) ; Niklas Wolff (ID) ; Fabian Lofink; Lorenz Kienle; Bernhard Wagner

🔴 Check for updates

Journal of Applied Physics

View Online

Export Citation

14 June 2024 04:45:23

AIP Publishing

AlScN: A III-V semiconductor based ferroelectric F

View Online   Export Citation   CrossMark

Simon Fichtner,[1,2,a)] iD Niklas Wolff,[3] iD Fabian Lofink,[2] Lorenz Kienle,[3] and Bernhard Wagner[1,2]

AFFILIATIONS

[1]Materials and Processes for Micro/Nanosystem Technologies, Institute for Material Science, University of Kiel, Kaiserstr. 2, 24143 Kiel, Germany
[2]Fraunhofer Institute for Silicon Technology (ISIT), Fraunhoferstr. 1, 25524 Itzehoe, Germany
[3]Synthesis and Real Structure, Institute for Material Science, University of Kiel, Kaiserstr. 2, 24143 Kiel, Germany

[a)]E-mail: sif@tf.uni-kiel.de

ABSTRACT

Ferroelectric switching is unambiguously demonstrated for the first time in a III-V semiconductor based material: $Al_{1-x}Sc_xN$—A discovery which could help to satisfy the urgent demand for thin film ferroelectrics with high performance and good technological compatibility with generic semiconductor technology which arises from a multitude of memory, micro/nano-actuator, and emerging applications based on controlling electrical polarization. The appearance of ferroelectricity in $Al_{1-x}Sc_xN$ can be related to the continuous distortion of the original wurtzite-type crystal structure towards a layered-hexagonal structure with increasing Sc content and tensile strain, which is expected to be extendable to other III-nitride based solid solutions. Coercive fields which are systematically adjustable by more than 3 MV/cm, high remnant polarizations in excess of 100 $\mu C/cm^2$—which constitute the first experimental estimate of the previously inaccessible spontaneous polarization in a III-nitride based material, an almost ideally square-like hysteresis resulting in excellent piezoelectric linearity over a wide strain interval from −0.3% to + 0.4% and a paraelectric transition temperature in excess of 600 °C are confirmed. This intriguing combination of properties is to our knowledge as of now unprecedented in the field of polycrystalline ferroelectric thin films and promises to significantly advance the commencing integration of ferroelectric functionality to micro- and nanotechnology, while at the same time providing substantial insight to one of the central open questions of the III-nitride semiconductors—that of their spontaneous polarization.

INTRODUCTION

Ferroelectrics possess a unit-cell originating spontaneous electrical polarization with a spatial orientation that can be altered from one stable direction to another under an applied electric field. This makes them a distinct class with increased functionality among the piezoelectric materials. The drive towards miniaturization of piezoelectric sensors and actuators (microelectromechanical systems, MEMS), the introduction of ferroelectric functionality into integrated circuit (IC-) technology, and numerous emerging applications based on polarization control have led to substantial scientific and commercial interest in ferroelectric thin films.[1–5] Many of the more important ferroelectrics are oxide perovskites, with typical disadvantages such as low paraelectric transition temperatures, non-linear displacements, or limited compatibility with, e.g., complementary metal-oxide-semiconductor (CMOS) or III-nitride technology—issues which so far impede the universal availability of ferroelectric functionality in microtechnology.[2,6]

In the wurtzite-type structure (space group $P6_3mc$), the III-V semiconductors AlN, GaN, and InN possess a spontaneous polarization along their c-axis, which originates in the separation of the group-III and nitrogen atoms in individual planes.[7] Therefore, two antiparallel polarization directions exist: N-polar and metal-polar (e.g., Ga- or Al-polar) [Fig. 1(a)]. The pure wurtzite-type III-nitrides are thus pyroelectric materials, but not ferroelectric, as it is accepted that their polarization direction cannot be switched with electric fields below their individual dielectric breakdown limit.[2] Due to the higher piezoelectric coefficients of AlN compared to GaN or InN, AlN is generally preferred for piezoelectric applications.[7,8] Akiyama et al. demonstrated that the piezoelectric response of solid solutions constituted from AlN and ScN increases monotonously with Sc content, as long as the wurtzite structure is maintained.[9,10] This can be related to a highly metastable layered-hexagonal phase (space group $P6_3/mmc$) in ScN,[11,12] which in turn flattens the ionic potential energy landscape of, e.g., wurtzite-type
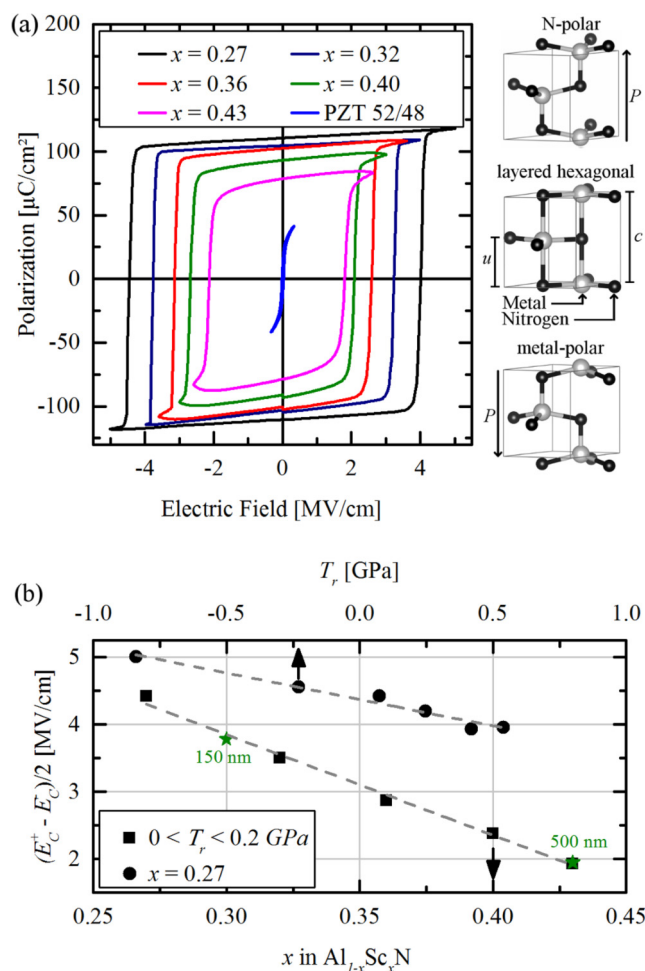
FIG. 1. (a) P-E loops of ferroelectric $Al_{1-x}Sc_xN$ with Sc contents of $x = 0.27$, 0.30, 0.32, 0.36, 0.40, and 0.43 as well as of PZT 52/48. To the right, the structures associated with the respective polarization states are displayed. (b) Dependence of the mean coercive field on the residual stress T_r and the Sc content of the $Al_{1-x}Sc_xN$ films. Sc content and T_r were varied independently.

$Al_{1-x}Sc_xN$. Consequently, the wurtzite basal plane as well as the internal parameter u (the length of the metal-nitrogen bond parallel to the c-axis relative to the lattice parameter c) increases, i.e., the layered hexagonal phase is approached, particularly at the Sc sites.[11,13,14] While the layered hexagonal structure itself is nonpolar, it can be seen as a transition state ($u = ½$) between the two polarization orientations of the wurtzite structure [Fig. 1(a)]. The sign of the polarization switches once u passes ½. Due to the flattening of the ionic potential towards the hexagonal structure, the energy barrier which is associated with $u = ½$ is set to decrease as the Sc content is increased. Strain engineering of the wurtzite basal plane should enable a further decrease of this barrier, as was predicted by Zhang et al. for $Ga_{0.625}Sc_{0.375}N$.[13] In the same case, the electric field necessary to achieve ferroelectric polarization

switching was also calculated to be potentially below the dielectric breakdown limit of pure GaN.[13] Aside from the incorporation of ScN into AlN, GaN, or InN, other metal nitrides such as YN or MgN-NbN were predicted and/or found to lead to a similar softening, increased a/c-lattice parameter ratio, or improved piezoelectric response.[12,13,15–17] The key to ferroelectric switching, however, remains that the energy barrier between the two polarization states of the wurtzite structure can be lowered sufficiently—either by increasing the ratio of the non-III metal or via strain engineering, while to some extent preserving the dielectric breakdown resistance of the pure III-nitride. In spite of this theoretical motivation, no experimental evidence of ferroelectric III-nitride semiconductors has been reported to date.

EXPERIMENTAL DETAILS

Polycrystalline $Al_{1-x}Sc_xN$ films were prepared by reactive sputter deposition on oxidized 200 mm (100) Si wafers covered with an AlN/Pt bottom electrode. The relevant process parameters for the $Al_{1-x}Sc_xN$ films deposited from dual targets (all except $Al_{0.64}Sc_{0.36}N$) were previously published.[18] $Al_{0.64}Sc_{0.36}N$ was deposited from a single alloy AlSc target with a nominal Sc content of 43 at. % and a purity of 99.9 at. %. Here, the DC power was set to 600 W, the gas flows into the chamber to 7.5 sccm of Ar and 15 sccm of N_2, while the substrate was kept at 400 °C during deposition. The film thickness was set to 400 nm (all films with $x = 0.27$), 600 nm ($x = 0.32$; 0.36; 0.40), or 1 μm ($x = 0.43$), unless stated explicitly. The lead zirconate titanate (PZT) film with a thickness of 600 nm was derived via solgel deposition with previously published process details.[19] (Piezo-) Electrical characterization took place on parallel plate capacitors with Pt top electrodes structured by lift-off. A commercially available aixACCT double beam laser interferometer (P-E loops, inverse piezoelectric effect, square 0.25 mm² top electrodes for P-E Loops, square 1 mm² top electrode for strain measurements) and a 4-point bending probe (direct piezoelectric effect, 16 mm² top electrodes) were used for the (piezo-) electric characterization.[20,21] P-E loops were measured with a triangular voltage input at 711 Hz and 411 Hz (for correction only, see the supplementary material). The inverse piezoelectric effect was measured with a triangular voltage input at 211 Hz. Due to systematic errors arising from non-neglectable substrate deformation during measurements of the inverse piezoelectric effect,[22] a correction factor of 0.85 was multiplied with the measured strain response (see the supplementary material). Permanent polarization inversion was initiated through a unipolar 0.1 Hz sine wave with a peak value of −200 V over 60 s. The residual stress was calculated via Stoney's equation based on capacitive measurements (E + H MX 203) and profilometer line scans (Ambios XP2) to extract the substrate curvature on the wafer level.[23] Temperature treatments were performed in consecutive steps of 5 min each under an ambient atmosphere. Etching experiments to resolve the polarity distribution in the $Al_{1-x}Sc_xN$ films were carried out in 85% phosphoric acid (H_3PO_4) and 25% potassium hydroxide (KOH) aqueous solutions at 80 °C. To remove the top electrodes after ex situ polarization inversion, ion beam etching (IBE, Oxford Instruments Ionfab 300) was employed. For the characterization of the micro- and nanostructure, transmission electron microscopy

was performed on three different microscopes during this investigation: Dark-field imaging was performed on a JEOL JEM-2100 (200 kV, LaB_6 cathode) while high-resolution TEM imaging was performed on a Tecnai F30 STwin microscope (300 kV, field emission cathode, $C_S = 1.2$ mm) and a Philips CM 30 ST (300 kV, LaB_6 cathode, CS = 1.15 mm). The cross-section sample was prepared by focused ion beam (FIB) milling using a standard lift-out method with a FEI Helios Nanolab system. The Sc content was measured by scanning electron microscopy energy dispersive x-ray spectroscopy (SEM-EDX) (Oxford x-act, 10 kV).

FERROELECTRIC PROPERTIES: POLARIZATION HYSTERESIS, DIRECT AND INDIRECT PIEZOELECTRIC EFFECT

Depending on the Sc content and the planar mechanical stress of the $Al_{1-x}Sc_xN$ films, it was possible to demonstrate not only that ferroelectric switching can indeed be achieved in wurtzite-type III-nitride based solid solutions—but also that the material has exceptional properties of relevance to the core-applications of ferroelectric thin films. The studied $Al_{1-x}Sc_xN$ layers generally exhibited good c-axis orientation normal to the substrate,[18] although grains with secondary orientations/phases were observed for Sc contents with $x \geq 0.4$ (see the supplementary material).

Distinct ferroelectric polarization inversion was measured starting at Sc contents of $x = 0.27$. Below $x = 0.22$, dielectric breakdown occurred before reaching the coercive field E_C. P-E (polarization over electric field) hysteresis loops of $Al_{1-x}Sc_xN$ with $x = 0.27$, 0.30, 0.32, 0.36, 0.40, and 0.43 are given in Fig. 1(a).

For comparison, the P-E loop of a $PbZr_{0.52}Ti_{0.48}O_3$ (PZT 52/48) film measured with the same parameters is displayed as well. To (at least partially) compensate the P-E loops with respect to the non-negligible leakage currents at higher electric fields, a modified dynamic leakage current compensation was employed (see the supplementary material).[24] In general, we observed very large coercive fields (close to 5 MV/cm at $x = 0.27$), almost undiminished polarization between the coercive fields and high remnant polarizations (110 $\mu C/cm^2$ at $x = 0.27$). The latter is significantly above most theoretical predictions of the spontaneous polarization in both pure AlN ($\approx 10\ \mu C/cm^2$) and $Al_{1-x}Sc_xN$ ($\approx 30\ \mu C/cm^2$ at $x = 0.5$), which were made using the zincblende structure as the reference.[7,25,26] The polarization and its trend to decrease with increasing Sc content (which in turn increases u and leads to approaching the non-polar layered hexagonal structure) are, however, in line with a more recent prediction made in reference to the layered hexagonal structure by Dreyer et al.[8] As such, it is a welcome side-effect of ferroelectricity in $Al_{1-x}Ax_xN$ that the previously experimentally virtually inaccessible spontaneous polarization of AlN can therefore projected to be indeed above 100 $\mu C/cm^2$, rather than below 10 $\mu C/cm^2$—thus providing an answer with regard to the uncertainty associated with the polarization constant of the III-nitrides and confirming the approach by Dreyer et al.

In addition to this theoretical prediction, the comparably large spontaneous polarization of AlN and $Al_{1-x}Sc_xN$ can also be motived based on its Born effective charge and ionic displacement. The Born effective charge Z^B of AlN is around 2.5 e,[7,14] while the ionic displacement Δd upon ferroelectric switching is twice

the nearest neighbour distance between metal and N-planes, i.e., $\Delta d = c(1 - 2u) = 1.2$ Å with $c = 5$ Å and $u = 0.38$.[9,13] While Z^B reportedly increases with increasing Sc content, Δd decreases due to an increasing internal parameter u—however, both values do not change dramatically until being energetically very close to the layered hexagonal phase (i.e., around x = 0.50).[13,14] While the effective ionic charge in $Al_{1-x}Sc_xN$ is thus not particularly large, the ionic displacement is 5-15 times above that of classical ferroelectric oxide perovskites like Barium- and Lead-Titanate.[27,28]

The polarization constant of AlN itself can be roughly approximated by

$$P = \frac{1}{2V}Z^B\Delta d =\ 126\,\mu C/cm^2, \tag{1}$$

where V is the volume per metal-nitrogen pair.[28] The so derived spontaneous polarization is close to the density functional theory-derived value of 135 $\mu C/cm^2$ for pure AlN[8] and motivates that, in spite of modest effective ionic charges, the large ionic displacements in ferroelectric $Al_{1-x}Sc_xN$ imply a spontaneous polarization above that of most other ferroelectrics.

The almost ideal box-like shape of the polarization hysteresis and the large coercive fields can be related to a still sizeable energy barrier associated with the hexagonal phase, good compositional homogeneity, and the wurtzite structure itself, which allows only 180° domain rotations. In terms of shape and polarization magnitude, the P-E loops of $Al_{1-x}Sc_xN$ remind of certain measurements on epitaxial ferroelectric thin films,[29–31] albeit without the need for a specific template to facilitate epitaxy and therefore with increased compatibility and ease of fabrication.

The gradual lowering of the switching barrier ($u = \frac{1}{2}$) with increasing Sc content results in a linear decline of the coercive field [Fig. 1(b)], from about 5 MV/cm ($Al_{0.73}Sc_{0.27}N$) to less than 2 MV/cm ($Al_{0.57}Sc_{0.43}N$). Just as the Sc content distorts the wurtzite-type crystal structure by expanding its basal plane and increasing u, lateral mechanical straining of the films can be used to the same end. Similar to what has been reported for pure AlN, permanent lateral mechanical stress of a well-defined magnitude was induced to the $Al_{1-x}Sc_xN$ films by varying the Ar partial pressure of the sputter gas.[32,33] Adjusting the mechanical stress T_r in $Al_{0.73}Sc_{0.27}N$ films from about −0.8 GPa to +0.5 GPa resulted in a linear decline of the coercive field by more than 1 MV/cm. Therefore, a high degree of flexibility exists to systematically adjust the switching voltage towards a value favoured for the intended application by independent variation of the residual stress or the Sc content. The range of achievable switching voltages is further extended by the observation that polycrystalline Al(Sc)N can possess a preferential c-axis orientation already on the first 10 nm from the substrate (see the supplementary material) and functional films of corresponding thicknesses are therefore feasible.[34] Thus, both high switching voltages (>100 V) of advantage to linear piezoelectric excitation and low switching voltages in ranges of relevance for memory applications (<10 V) could be realized.

Measurements of the direct and inverse piezoelectric effect in ferroelectric $Al_{0.64}Sc_{0.36}N$ are given in Figs. 2(a) and 2(b), respectively. Both directions imply the possibility for virtually complete
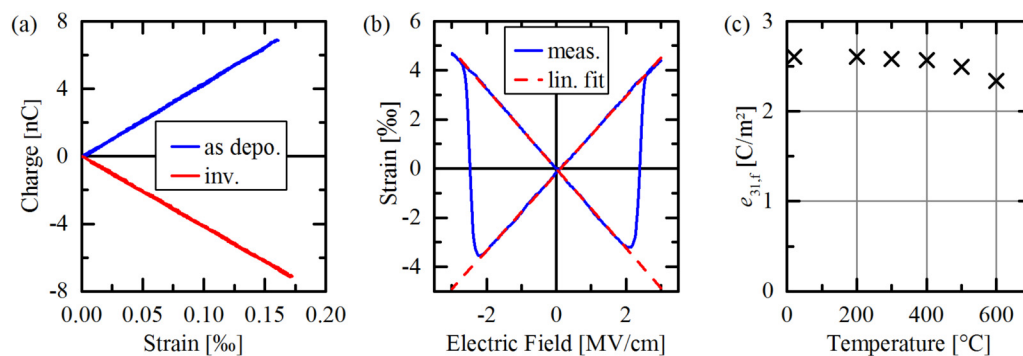
FIG. 2. (a) Direct piezoelectric effect: Charge-strain curves of $Al_{0.64}Sc_{0.36}N$ as deposited and after ferroelectric polarization inversion. (b) Converse piezoelectric effect: Longitudinal strain response of $Al_{0.64}Sc_{0.36}N$. (c) Transverse piezoelectric coefficient after polarization inversion and successive temperature treatments at the indicated temperatures without subsequent repolarization.

polarization inversion during ferroelectric switching. For measurements of the direct piezoelectric effect on an inverted sample, a simple 1-min poling procedure at room temperature was used to switch between the polarization states. Under this procedure, the effective transverse piezoelectric coefficient $e_{31,f}$ was inverted from an as-deposited $-2.90\,C/m^2$ to $2.76\,C/m^2$. Both values can be considered high for an AlN-based solid solution.[18,35] Repeated measurements of the piezoelectric response up to 30 weeks after polarization inversion did not show measurable degradation.

Moreover, the polarization inversion was conserved up to at least 600 °C: $e_{31,f}$ declined only slightly during the temperature treatment steps [Fig. 2(c)]. Consequently, 600 °C can be seen as a lower limit for the paraelectric transition temperature of $Al_{0.64}Sc_{0.36}N$. Beyond 600 °C, a degradation of the electrodes prohibited further electrical characterization of the capacitors.

The longitudinal displacement butterfly curve [Fig. 2(b)] of the inverse piezoelectric effect has broad linear regimes with almost equal slopes which correspond to an effective longitudinal piezoelectric coefficient $d_{33,f}$ of 15.7 pm/V and -16.2 pm/V. Compared to state of the art polycrystalline ferroelectric thin-films, both the width of the linear strain regime of 0.7% and its symmetry around the field axis are outstanding.[36]

ADDITIONAL EVIDENCE FOR GENUINE FERROELECTRICITY ASSOCIATED WITH THE WURTZITE CRYSTAL STRUCTURE

It is long known that not only true ferroelectricity results in P-E hysteresis loops, but also electrets, finite conductance, or p-n and Schottky junctions can lead to P-E measurements which resemble ferroelectricity.[3,37–40] In contrast to these spurious effects, which are connected with charge migration on length scales up to the film thickness, ferroelectricity is based on a stable and repeatable polarization reorientation on unit-cell level. The ultimate evidence for ferroelectric switching would therefore be the *in situ* observation of the underlying atomic displacement under and after the application of an external electric field. While such experiments were performed in the past,[41] the high coercive fields of AlScN

would add additional challenge to an already demanding investigation. Alternatively, *ex situ* polarization inversion could be used with methods where the contrast specific for the unit-cell orientation can be obtained between pristine regions and switched regions. For the case of the wurtzite semiconductors GaN, AlN, InN, and ZnO, a standard method which provides such unit-cell orientation specific contrast is wet-etching in both acid (H_3PO_4) and bases like aqueous KOH and tetramethyl ammonium hydroxide (TMAH).[42–48] While N-polar surfaces etch readily and with distinct residues, metal polar surfaces do barely etch at all and initially remain smooth, with the exception of local defects and inversion domains.

To investigate whether this anisotropy can be observed in $Al_{1-x}Sc_xN$, samples from the same wafer as used for the piezoelectric characterization above had some of their capacitors switched, while others were kept as deposited. Subsequently, their top electrode was removed via IBE with an intentional 50 nm overetch into the $Al_{0.64}Sc_{0.36}N$ film [Fig. 3(a)]. This overetch was chosen in order to, on the one hand, rule out masking due to residues of the top electrode and, on the other hand, remove the interface region of the $Al_{0.64}S_{0.36}N$ film, as charge injection and ionic migration typically manifest around the electrodes.[38,39] Afterwards, the samples were etched in H_3PO_4 and KOH until not more than residues remained on the bottom electrode outside the capacitor areas. After wet etching, polarization inverted structures were conserved with close to their full height (ca. 500 nm), having a smooth surface intermitted by deep holes due to either defects or non-switching inversion domains [Fig. 3(b)] [the presence of the latter can be assumed due to the slightly lower inverted piezoelectric coefficient of the samples, Fig. 2(a)], which merged after longer etching times in H_3PO_4 or when etching in KOH, because of generally more rapid etching in the latter case. Due to this lateral etching, even small defect regions can account for the observed pits on the metal-polar surface. Asides from the metal polar-surface, the rest of the film etched readily and with the characteristic, cone like residues [Fig. 3(c)]. Due to the comprehensive investigation of the same effect in pure wurtzite semiconductors, this result provides conclusive evidence that polarization switching on unit-cell level does indeed take place in $Al_{1-x}Sc_xN$ and that, therefore, the material is a genuine ferroelectric.
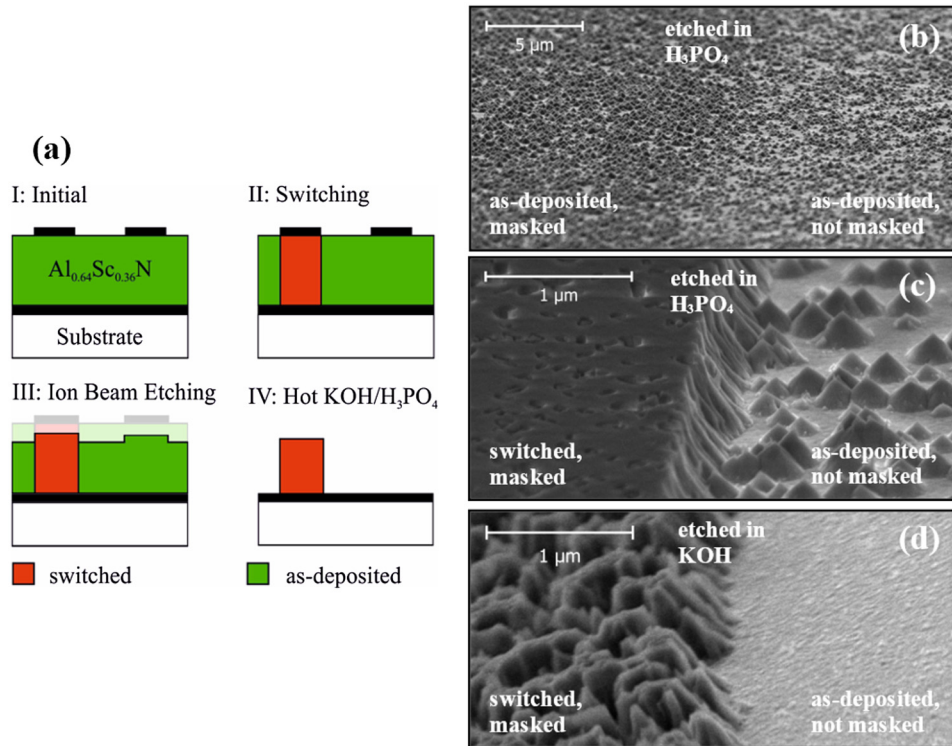
FIG. 3. (a) Sketch of the experimental procedure to determine the polarity of $Al_{0.64}Sc_{0.36}N$ via wet etching. (b) SEM image of the step from a masked, as deposited, region to an unmasked as-deposited region (faintly visible as a line through the center of the image) after etching in H_3PO_4 for 5 min. (c) Step from a switched region to an as-deposited region after etching in H_3PO_4 for 5 min. (d) Step from a switched region to an as-deposited region after etching in KOH for 15 s.

Additional evidence for ferroelectricity in $Al_{1-x}Sc_xN$ can be obtained from retention and frequency dependent measurements of the electrical polarization. Unlike the measured coercive field, the measured switching polarization of a true ferroelectric material should be largely independent of the measurement frequency. Due to $\Delta P \sim \int I(t)\,dt$, where $I(t)$ is the measured current during sweeping of the electric field, the extrema of the former have to be approximately proportional to frequency (or more precisely, the area under its peaks has to be). This is typically not the case for currents due to charge injection/leakage, which either stay constant or decrease for increasing frequencies.[24,38] For $Al_{1-x}Sc_xN$, the area associated with the switching current peaks does scale proportionally with frequency over more than two orders of magnitude and the measured switching polarization consequently is constant (see the supplementary material)—as one would expect of a proper ferroelectric.
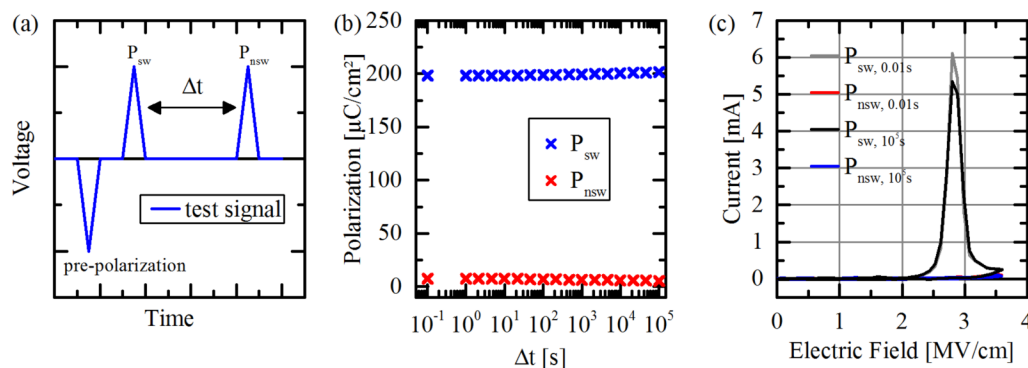

FIG. 4. (a) Pulse sequence to determine the retention behaviour of $Al_{1-x}Sc_xN$ via switching and non-switching polarization measurements (P_{sw}, P_{nsw}) separated by a time Δt during which the capacitor was shortened. The pulse width is 2 ms. (b) Switching and non-switching polarization over retention time Δt. (c) Initial and final current measurements, from which P_{sw} and P_{nsw} were extracted—a slight increase due to leakage current can be observed in the non-switching current for high electric fields, contributing to the non-zero non-switching polarization which is therefore not due to true polarization switching.

Furthermore, the stability of the polarization in electrets due to injected charges over time has the tendency to be lower than those of ferroelectrics (although there are exceptions).[37] The retention behavior of $Al_{0.64}Sc_{0.36}N$ was therefore determined by using the voltage pulse sequence given in Fig. 4(a). In between the read pulses for the switching (P_{sw}) and non-switching polarization (P_{nsw}), the capacitor was shortened. Over 10^5 s, no polarization loss that could be attributed to polarization back switching was observed [Fig. 4(b)]. The fact that P_{nsw} is still not exactly zero appears to be rather due to purely dielectric effects [leakage and polarization magnitude, Fig. 4(c)]. The typical linear loss of polarization after ferroelectric switching which was observed over a logarithmic time scale in other materials[37,49] could not be observed in $Al_{1-x}Sc_xN$, although orders of magnitude longer measurements would be necessary to give a more definite understanding of the polarization retention in $Al_{1-x}Sc_xN$. It is, however, straightforward to motivate an exceptionally long retention time in $Al_{1-x}Sc_xN$, based not only on the current retention measurements but also on the fact that in its parent material, AlN, polarization is considered to be permanently aligned.

Asides from providing evidence that actual ferroelectric switching on unit-cell level does take place, transmission electron microscopy (TEM) was employed to confirm that the wurtzite structure is indeed conserved during the application of a switching field and no previously unconsidered phase is induced. In this context, an $Al_{0.57}Sc_{0.43}N$ TEM sample was prepared such that it contains two regions: one being sandwiched by Pt electrodes and subjected to ferroelectric polarization inversion and an unaltered region to allow for a structural comparison. An illustration of stitched TEM dark field images mapping out the intensity of the wurtzite-type $Al_{0.57}Sc_{0.43}N$ (0002) reflection is given in Fig. 5(a) with the precession electron diffraction (PED) pattern of the wurtzite structure in Fig. 5(b). No significant difference in contrast between crystal columns below the Pt top electrode used for polarization inversion and crystal columns not subjected to the switching electric field was observed.

From electron diffraction experiments, the majority of the film was identified as (0002) textured $Al_{1-x}Sc_xN$, in both the pristine and the polarization-inverted regions. Therefore, ferroelectricity in $Al_{1-x}Sc_xN$ can indeed be related to the wurtzite-type structure. However, owned to the high Sc content of the particular sample, a number of misoriented wurtzite grains were identified, some of which are marked by asterisks in Fig. 5(a). Moreover, small structural variations in the form of potential cubic grains and an unidentified phase were occasionally observed. Although being of high interest,
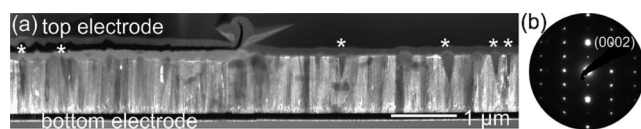
the transition towards a layered hexagonal structure itself cannot be retrieved from precession electron diffraction data alone—kinematic simulations suggest that the contrast between the polar and non-polar phases can hardly be differentiated at a Sc content of $x = 0.43$. These aspects are discussed in more detail within the supplementary material.

CONCLUSION

In summary, ferroelectric switching could be demonstrated in $Al_{1-x}Sc_xN$, beginning at Sc concentrations of $x = 0.27$. We expect that this material is only the first of a new group of ferroelectric wurtzite-type III-nitride based solid solutions, with likely additional candidates for this class being, e.g., $Ga_{1-x}Sc_xN$, $Al_{1-x}Y_xN$, or $Al_{1-x-y}Mg_xNb_yN$. Ferroelectric switching allowed the first direct experimental observation of the switching spontaneous polarization in an AlN based material and confirmed that, contrary to most prior theoretical publications, it can reach values larger than $100\,\mu C/cm^2$. The unique combination of ferroelectric properties of $Al_{1-x}Sc_xN$ in concert with the excellent compatibility to existing technology platforms should make the material highly relevant for both the classical applications of ferroelectrics, like piezoelectric multilayer actuator stacks or non-volatile memory cells and for novel approaches based on controlling electrical polarization, e.g., in the fields of optoelectronics, multiferroic composites, and III-nitride technology.[1,4,5,25]

SUPPLEMENTARY MATERIAL

See the supplementary material for a discussion of the leakage current as well as longitudinal strain correction, frequency dependent measurements of the switching current, additional SEM images illustrating the sample morphology, and a more in-depth TEM analysis of the microstructure of $Al_{0.57}Sc_{0.43}N$.

FIG. 5. (a) TEM darkfield image mapping out the intensity of the (0002) reflection indicated in the PED pattern (b). Misoriented crystals that do not exhibit the wurtzite-type (0002) texture of the matrix are displayed with a darker contrast in the brighter crystal matrix and are partially indicated by (*).

REFERENCES

[1]N. Setter, D. Damjanovic, L. Eng, G. Fox, S. Gevorgian, S. Hong, A. Kingon, H. Kohlstedt, N. Y. Park, G. B. Stephenson, I. Stolitchnov, A. K. Taganstev, D. V. Taylor, T. Yamada, and S. Streiffer, J. Appl. Phys. **100**, 51606 (2006).

[2]P. Muralt, R. G. Polcawich, and S. Trolier-Mckinstry, MRS Bull. **35**, 658 (2009).

[3]M. Dawber, K. M. Rabe, and J. F. Scott, Rev. Mod. Phys. **77**, 1083 (2005).

[4]Y. Zhang, W. Jie, P. Chen, W. Liu, and J. Hao, Adv. Mater. **30**, 1707007 (2018).

[5]J. Ma, J. Hu, Z. Li, and C. W. Nan, Adv. Mater. **23**, 1062 (2011).

[6]S. Zhang, R. Xia, L. Lebrun, D. Anderson, and T. R. Shrout, Mater. Lett. **59**, 3471 (2005).

[7]F. Bernardini, V. Fiorentini, and D. Vanderbilt, Phys. Rev. B **56**, R10 024 (1997).

[8]C. E. Dreyer, A. Janotti, C. G. Van de Walle, and D. Vanderbilt, Phys. Rev. X **6**, 021038 (2016).

[9]M. Akiyama, T. Kamohara, K. Kano, A. Teshigahara, Y. Takeuchi, and N. Kawahara, Adv. Mater. **21**, 593 (2009).

[10]M. Akiyama, K. Kano, and A. Teshigahara, Appl. Phys. Lett. **95**, 162107 (2009).

[11]F. Tasnadi, B. Alling, C. Höglund, G. Wingqvist, J. Birch, L. Hultman, and I. A. Abrikosov, Phys. Rev. Lett. **104**, 137601 (2010).

[12]N. Farrer and L. Bellaiche, Phys. Rev. B **66**, 2012031 (2002).

[13]S. Zhang, D. Holec, W. Y. Fu, C. J. Humphreys, and M. Moram, J. Appl. Phys. **114**, 133510 (2013).

[14]R. Deng, K. Jiang, and D. Gall, J. Appl. Phys. **115**, 13506 (2014).

[15]C. Tholander, J. Birch, F. Tasnádi, L. Hultman, J. Pališaitis, P. O. Å. Persson, J. Jensen, P. Sandström, B. Alling, and A. Žukauskaitė, Acta Mater. **105**, 199 (2016).

[16]P. M. Mayrhofer, H. Riedl, H. Euchner, M. Stöger-Pollach, P. H. Mayrhofer, A. Bittner, and U. Schmid, Acta Mater. **100**, 81 (2015).

[17]M. Uehara, H. Shigemoto, Y. Fujio, T. Nagase, Y. Aida, K. Umeda, and M. Akiyama, Appl. Phys. Lett. **111**, 112901 (2017).

[18]S. Fichtner, N. Wolff, G. Krishnamurthy, A. Petraru, S. Bohse, F. Lofink, S. Chemnitz, H. Kohlstedt, L. Kienle, and B. Wagner, J. Appl. Phys. **122**, 35301 (2017).

[19]A. Piorra, R. Jahns, I. Teliban, J. L. Gugat, M. Gerken, R. Knöchel, and E. Quandt, Appl. Phys. Lett. **103**, 32902 (2013).

[20]K. Prume, P. Muralt, F. Calame, T. Schmitz-Kempen, and S. Tiedke, IEEE Trans. Ultrason. Ferroelectr. Freq. Control **54**, 8 (2007).

[21]P. Gerber, A. Roelofs, O. Lohse, C. Kügeler, S. Tiedke, U. Böttger, and R. Waser, Rev. Sci. Instrum. **74**, 2613 (2003).

[22]S. Sivaramakrishnan, P. Mardilovich, T. Schmitz-Kempen, and S. Tiedke, J. Appl. Phys. **123**, 14103 (2018).

[23]G. C. A. M. Janssen, M. M. Abdalla, F. van Keulen, B. R. Pujada, and B. van Venrooy, Thin Solid Films **517**, 1858 (2009).

[24]R. Meyer, R. Waser, K. Prume, T. Schmitz, and S. Tiedke, Appl. Phys. Lett. **86**, 142907 (2005).

[25]O. Ambacher, J. Smart, J. R. Shealy, N. G. Weimann, K. Chu, M. Murphy, W. J. Schaff, L. F. Eastman, R. Dimitrov, L. Wittmer, M. Stutzmann, W. Rieger, and J. Hilsenbeck, J. Appl. Phys. **85**, 3222 (1999).

[26]M. Caro, S. Zhang, T. Riekkinen, M. Ylilammi, M. Moram, O. Lopez-Acevedo, J. Molarius, and T. Laurila, J. Phys. Condens. Matter **27**, 245901 (2015).

[27]R. E. Cohen, Nature **358**, 136 (1993).

[28]P. Ghosez, J. Michenaud, and X. Gonze, Phys. Rev. B **58**, 6224 (1998).

[29]H. W. Jang, S. H. Baek, D. Ortiz, C. M. Folkman, C. B. Eom, Y. H. Chu, P. Shafer, R. Ramesh, V. Vaithyanathan, and D. G. Schlom, Appl. Phys. Lett. **92**, 062910 (2008).

[30]I. Vrejoiu, G. Le Rhun, L. Pintilie, D. Hesse, M. Alexe, and U. Gösele, Adv. Mater. **18**, 1657 (2006).

[31]J. Karthik, A. R. Damodaran, and L. W. Martin, Adv. Mater. **24**, 1610 (2012).

[32]S. Fichtner, T. Reimer, S. Chemnitz, F. Lofink, and B. Wagner, APL Mater. **3**, 116102 (2015).

[33]M.-A. Dubois and P. Muralt, J. Appl. Phys. **89**, 6389 (2001).

[34]U. Zaghloul and G. Piazza, Appl. Phys. Lett. **104**, 253101 (2014).

[35]S. Mertin, B. Heinz, O. Rattunde, G. Christmann, M.-A. Dubois, S. Nicolay, and P. Muralt, Surf. Coat. Technol. **343**, 2–6 (2018).

[36]B. Narayan, J. S. Malhotra, R. Pandey, K. Yaddanapudi, P. Nukala, B. Dkhil, A. Senyshyn, and R. Ranjan, Nat. Mater. **17**, 427 (2018).

[37]J. F. Scott, C. A. Araujo, H. B. Meadows, L. D. McMillan, and A. Shawabkeh, J. Appl. Phys. **66**, 1444 (1989).

[38]L. Pintilie and M. Alexe, Appl. Phys. Lett. **87**, 112903 (2005).

[39]J. F. Scott and P. Zubko, in *12th International Symposium on Electrets*, Salvador, Brazil, 11-14 September 2005 (IEEE, New York, 2005), p. 113.

[40]J. F. Scott, J. Phys. Condens. Matter **20**, 21001 (2008).

[41]P. Gao, C. T. Nelson, J. R. Jokisaari, S. H. Baek, C. W. Bark, Y. Zhang, E. Wang, D. G. Schlom, C. B. Eom, and X. Pan, Nat. Commun. **2**, 591 (2011).

[42]P. Visconti, D. Huang, M. A. Reshchikov, F. Yun, R. Cingolani, D. J. Smith, J. Jasinski, W. Swider, Z. Liliental-Weber, and H. Morkoç, Mater. Sci. Eng. B **93**, 229 (2002).

[43]J. Jasinski, Z. Liliental-Weber, Q. S. Paduano, and D. W. Weyburne, Appl. Phys. Lett. **83**, 2811 (2003).

[44]M. Bickermann, S. Schmidt, B. M. Epelbaum, P. Heimann, S. Nagata, and A. Winnacker, J. Cryst. Growth **300**, 299 (2007).

[45]D. Zhuang and J. H. Edgar, Mater. Sci. Eng. R Reports **48**, 1 (2005).

[46]A. N. Mariano and R. E. Hanneman, J. Appl. Phys. **34**, 384 (1963).

[47]E. S. Hellman, MRS Internet J. Nitride Semicond. Res. **3**, 1 (1998).

[48]E. Milyutin, S. Harada, D. Martin, J. F. Carlin, N. Grandjean, V. Savu, O. Vaszquez-Mena, J. Brugger, and P. Muralt, J. Vac. Sci. Technol. B **28**, L61 (2010).

[49]X. J. Lou, J. Appl. Phys. **105**, 024101 (2009).